Influences of Self-Assembled Structure on Mobilities of Charge Carriers in π-Conjugated Polymers

ARTICLE *in* THE JOURNAL OF PHYSICAL CHEMISTRY B · FEBRUARY 2005

Impact Factor: 3.3 · DOI: 10.1021/jp0460994 · Source: PubMed

Influences of Self-Assembled Structure on Mobilities of Charge Carriers in π-Conjugated Polymers

Xiaoqing Jiang, Rahul Patil, Yutaka Harima,* Joji Ohshita, and Atsutaka Kunai

Graduate School of Engineering, Hiroshima University, 1-4-1 Kagamiyama, Higashi-Hiroshima 739-8527, Japan

Received: August 29, 2004; In Final Form: October 20, 2004

Mobilities of charge carriers in cast and spun films of poly(3-hexylthiophene)s (PHTs) with regioregularities of 97%, 81%, 70%, and 54% (denoted as PHT97%, PHT81%, PHT70%, and PHT54%, respectively) are evaluated as a function of doping level. A common feature of mobility vs doping level plots for all the PHT films is that the mobility decreases initially with the increase of the doping level and then starts to rise drastically at ca. 1% doping level. No large mobility difference is observed between cast and spun films of each PHT. In contrast, the difference in regioregularity of PHT resulted in a large mobility difference, especially in the low doping regime. At the highest doping levels of ca. 20%, the apparent mobility values reach 0.4 and 0.01 $cm^2\ V^{-1}\ s^{-1}$ for the cast films of PHT97% and PHT54%, respectively. These features of the mobility plots are discussed in connection with self-assembled structures of PHT films studied by electrochemical, in-situ ESR, in-situ UV−vis−NIR, and X-ray diffraction measurements. It is concluded first that mobilities of polarons are mainly controlled by the rate of an interchain charge hopping and second that the evolution of metallic conduction featured by the sharp mobility increase is irrelevant to the interchain stacking, or rather governed by an intrachain route.

1. Introduction

Conducting π-conjugated polymers have attracted considerable attention owing to their interesting properties as well as their promise for providing new materials for modern technologies such as organic light emitting diodes, field effect transistors, optical converters, or molecular switches.[1,2] Among various conducting polymers, poly(3-alkylthiophene)s (PATs) have been investigated intensively due to their high conductivities, environmental stabilities and high solubilities.[3] One of the most important properties characteristic of PATs is regioregularity, which denotes the percentage of stereoregular head-to-tail (HT) attachments of the alkyl side chains to the 3-position of the thiophene rings.[4] Side chains of adjacent rings in PAT can be in head to tail (HT) or in head to head (HH) conformation, resulting in four triad regioisomers: HT-HT, HT-HH, TT-HT, and TT-HH triad. PATs with only HT-HT triad (regioregular PATs) lead to a minimal steric hindrance and an extended π-conjugation length as a result of self-organization of PAT main chains, whereas the HH or TT junctions result in spatially disordered polymer chains with limited conjugated segments.[4,5] In regioregular PAT films, the main chains stack on top of each other and the alkyl side chains extend the space between neighboring main chain stacks. The microstructure in a PAT film can be controlled by the change in regioregularity of PAT. It has been reported further that additional long-range ordered structures exist in regioregular PAT films[5] and the regioregular PAT forms larger and better ordered regions than less regioregular PAT.[6] The degree of self-ordering and orientation of the stacks is also known to depend greatly on the film preparation technique.[7−10]

Several mobility studies with PAT films have already been made and high mobilities up to 0.1 $cm^2\ V^{-1}\ s^{-1}$ are reported for regioregular PAT films.[7,11−13] All of these studies on mobilities, however, use either field-effect-transistor (FET) or time-of-flight (TOF) technique with undoped PAT films as a sample. Mobilities as well as conductivities in conducting polymer films are known to depend greatly on the doping level[14−16] and changes in mobility with the doping level, in particular, give useful information on the transport mechanisms in conducting polymers. Up to the present time, no report except one made by us on regioregular poly(3-octylthiophene)[16] deals with the measurements of mobilities in PAT films at various oxidation stages. Undoubtedly, the reason for this lies in the difficulty in application of the FET and TOF techniques to the doped and thus conducting PAT films.

In the present study of cast or spun films of poly(3-hexylthiophene)s (PHTs) with different regioregularities, influences of microstructure of conducting polymers on their transport properties are investigated by use of in-situ techniques. Mobilities are determined as a function of doping level. This technique, which is a combination of in-situ conductivity measurement and potential-step chronocoulometry, allows us to measure mobilities over a range of doping level.[14−17] In-situ UV−vis−NIR and in-situ ESR measurements are also carried out to characterize charge carriers in the polymer films at various doping levels. X-ray diffraction measurements are also made with the neutral PAT films for comparing morphologies of different films.

2. Experimental Section

Regioregular and regiorandom PHTs were obtained from Aldrich. Regioregularities of these PHTs were determined as 97% and 54% by ^{1}H NMR. Hereafter, the regioregular and regiorandom PHT will be denoted as PHT97% and PHT54%, respectively. PHTs with regioregularities of 81% and 70% were

* Corresponding author. E-mail: harima@mls.ias.hiroshima-u.ac.jp.

10.1021/jp0460994 CCC: $30.25
Published on Web 12/10/2004

synthesized by oxidative coupling of 3-hexylthiophene with $FeCl_3$.[18] These four PHTs obtained from two different sources showed a systematic change in the shape of absorption spectrum: absorption maxima for PHT97%, PHT81%, PHT70%, and PHT54% in chloroform were 457, 442, 434, and 431 nm and those for spun films were 545, 498, 479, and 449 nm, respectively. Thin films of PHTs were prepared onto Pt-coated glasses by casting or spin-coating of chloroform solutions. When spun films of PHT97% being prepared, however, hot tetrahydrofuran was used as solvent because PHT97% was not completely dissolved in chloroform at concentrations beyond 10 mg cm^{-3}. Electrochemical measurements were carried out using a three-electrode system in acetonitrile (CH_3CN) containing 0.1 M tetraethylammonium perchlorate (Et_4NClO_4) under N_2 atmosphere. Conductivities (σ) and doping levels were in-situ measured by a two-probe method and a potential-step chronocoulometry, respectively.[14−17] The experimental setup for simultaneous measurements of both quantities is illustrated in Figure 2 of ref 17. The doping level is defined as the number of charges per thiophene ring. Two-probe conductivity measurements were carried out using two kinds of electrodes. One is a two-band electrode made up of two Pt sheets of 0.1 mm thickness. [19] It was used in the high doping region where resistances of PHT films were low. In the low doping region, the other electrode, a microarray Pt electrode (100 lines, 20 μm spacing, 50 cm in total width), was employed because the film resistances were too high to be measured with the conventional two-band electrode. The latter electrode was unable to be used in the high doping region where the polymer resistances were comparable with or lower than the electrode resistance. Resistance vs potential plots obtained with the two kinds of electrodes were compared and a potential region where slopes of the plots were close to each other was sought. Conductivities in this potential region were assumed to be the same for both the electrodes and a unified conductivity vs potential plot was obtained by combining two sets of resistance data. The resistances were converted to conductivities on the basis of the thickness of a polymer film and geometries of the electrodes. To confirm a negligible influence of the contact resistance at the Pt/polymer junction on the resistances measured with the two-probe method, the in-situ four-probe was applied for PHT97% film at moderately and heavily doped states. Details of the in-situ four-probe conductivity measurements will be described elsewhere. Apparent mobilities of charge carriers (μ) in the PHT films at various potentials or doping levels were evaluated from the equation $\mu = \sigma/ne$ for a single carrier model, where n is the density of charge carriers and e is the electronic charge. Film densities of PHTs were assumed to be 1 g cm^{-3} in calculating the carrier density n from the doping level. In-situ absorption spectra were taken using an airtight thin layer cell (5 mm in optical path length) with ITO as the counter electrode and the Ag/Ag^+ reference electrode in a separate compartment. Sample solution was transferred into the thin layer cell with a syringe. In-situ ESR measurements were performed as described earlier.[20] Intensities and magnetic fields of the ESR spectra of the PHT films were calibrated by simultaneously measuring ESR spectra of Mn^{2+} in MgO as an external standard. The absolute spin numbers were determined by referring to a standard sample of 1,1′-diphenyl-2-picrylhydrazyl (DPPH) in benzene. All the measurements were performed at room temperature under N_2 atmosphere. X-ray diffraction profiles were measured using a JEOL JDX-11RA rotation anode type X-ray diffractometer. The X-ray beam was Cu Kα radiation operated at 40 kV and 140 mA. Data were obtained from 3° to 30° (2θ) at 0.005° s^{-1}.

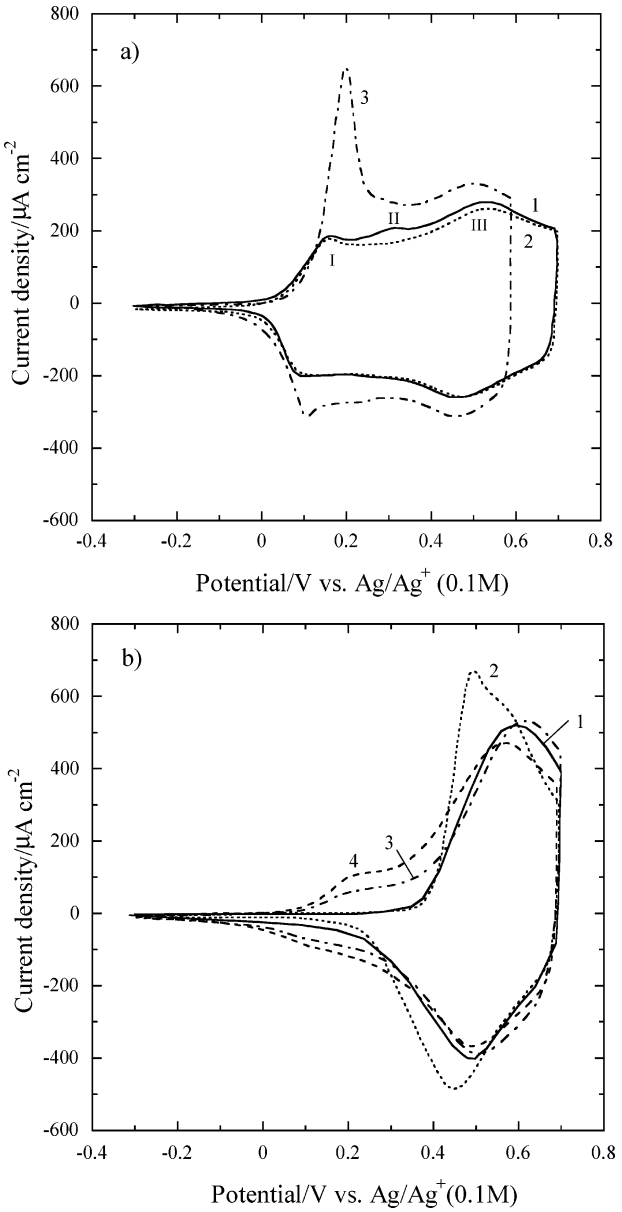

Figure 1. (a) Cyclic voltammograms for (1) cast, (2) spun, and (3) multi-dip-cast films of PHT97%. (b) Cyclic voltammograms for (1) cast and (2) spun films of PHT54%, and cast films of (3) PHT70% and (4) PHT81%. Solution is CH_3CN/Et_4NClO_4 (0.1 M) and potential-sweep rate is 100 mV s^{-1}.

3. Results

3.1. Electrochemistry Measurements. Figure 1 depicts typical cyclic voltammograms (CVs) for cast and spun films of PHTs with different regioregularities in CH_3CN containing 0.1 M Et_4NClO_4. In Figure 1a for PHT97% films, curve 1 is obtained for a drop-cast film, curve 2 for a spun film, and curve 3 for a dip-cast film. PHT97% films prepared by these techniques usually exhibited three pairs of redox waves with oxidation/reduction peak potentials at around 0.16/0.10 V, 0.30/0.25 V, and 0.51/0.45 V (shown by peaks I, II, and III in curve 1, respectively), although peak II was not seen in some experimental runs. Heights of peaks I and II changed considerably from film to film. However, no obvious systematic distinction in the CV shape between drop-cast and spun films

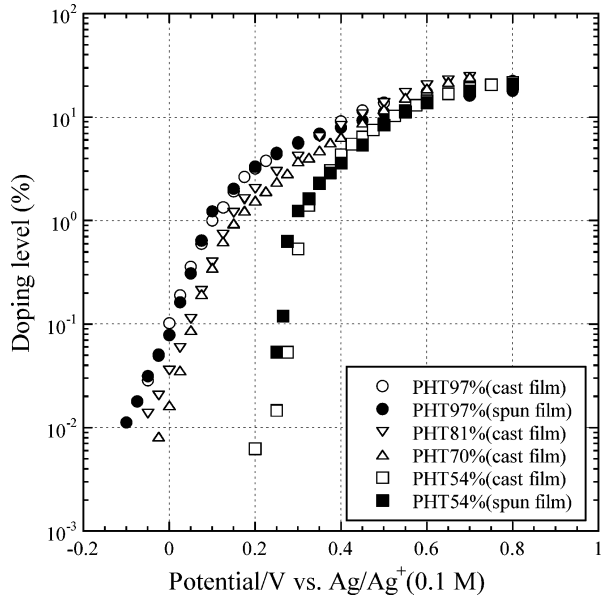

Figure 2. Doping levels of cast films of PHT97% (○), PHT81% (▽), PHT70% (△), and PHT54% (□) and spun films of PHT97% (●) and PHT54% (■) as a function of potential.

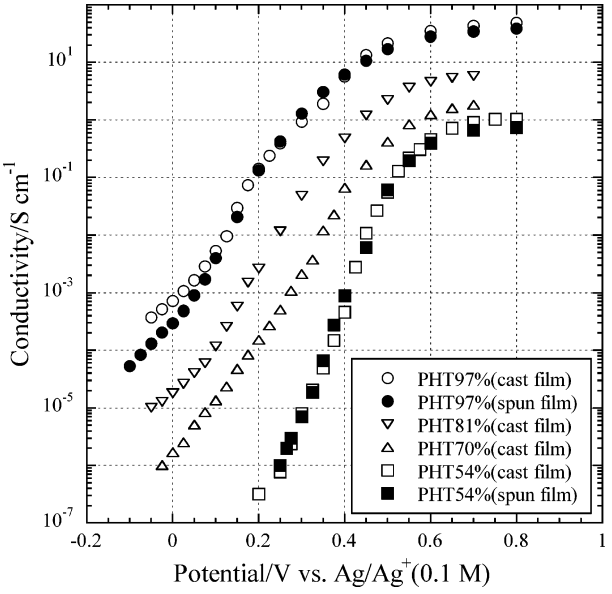

Figure 3. In-situ conductivities of cast films of PHT97% (○), PHT81% (▽), PHT70% (△), and PHT54% (□) and spun films of PHT97% (●) and PHT54% (■) as a function of potential.

was observed. As shown in curve 3, peak I at around 0.16−0.2 V is very sharp when the PHT97% film with uniform and shiny surface is prepared by dipping the electrode several times in a 15 mg cm^{-3} chloroform solution of PHT97%. In contrast to PHT97%, no peak can be seen at potentials less positive than 0.3 V in the CV curves for PHT54% films in Figure 1b, where curve 1 is obtained with a drop-cast film, and curve 2 with a spun film. CVs of PHT54% films sometimes show a prepeak, which becomes prominent or even shifts to a less positive potential and becomes a separate one when the potential-sweep rate is decreased. The CV curve for the cast film of PHT81%, shown by curve 4 in Figure 1b, exhibits two oxidation peaks at 0.2 and 0.6 V. For the cast film of PHT70%, oxidation peaks appear at potentials similar to those for the PHT81% film, although the peak height at 0.2 V is smaller than the one for the PHT81% film. The redox wave at 0.5−0.6 V is always observed irrespective of the difference in the sample regioregularity or in the preparation method of PHT films.

Doping levels for cast and spun films of PHT97% and PHT54%, and for cast films of PHT81% and PHT70% are plotted in Figure 2 as a function of potential. Doping and dedoping charges coincided well within experimental errors below 5% in the whole potential range investigated, and they were very reproducible. The doping level plots depend greatly on the sample regioregularity but are almost independent of the film preparation methods as shown in Figure 2. The doping level for cast and spun films of PHT54% increases more sharply and at more positive potential than those for PHT97% films. For all the films including cast fims of PHT81% and PHT70%, doping levels level off when the potential exceeds 0.6 V and reaches 21−25%. These values compare well with the maximum doping levels of 20−26% reported for heavily doped PAT films.[14−16]

Figure 3 represents in-situ conductivities for cast and spun films of PHT97% and PHT54% plotted against potential, together with similar plots for cast films of PHT81% and PHT70%. No large difference is seen again between cast and spun films except for in the low potential regime for PHT97% films. Conductivities for all the films increase steadily as the potential increases and level off at potentials beyond 0.6 V. Plots

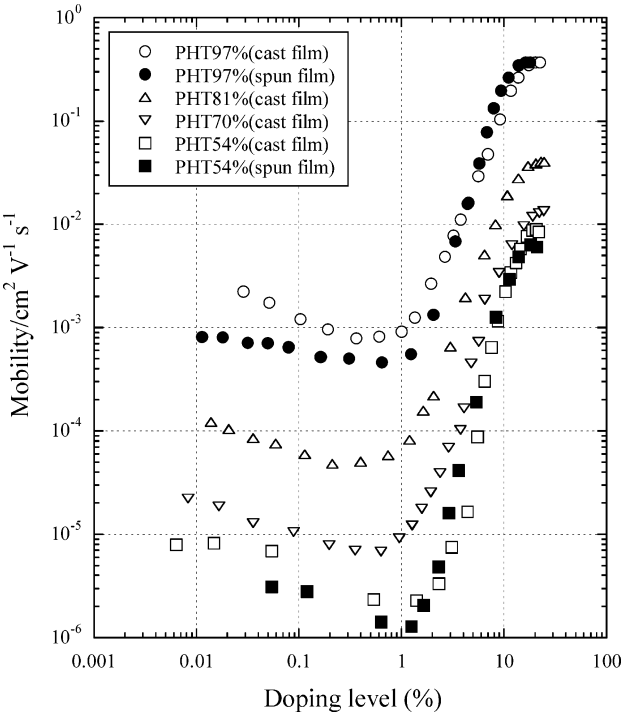

Figure 4. Apparent mobilities of charge carriers in cast films of PHT97% (○), PHT81% (▽), PHT70% (△), and PHT54% (□) and in spun films of PHT97% (●) and PHT54% (■) as a function of doping level.

for PHT films with smaller regioregularity values are shifted to more anodic direction, consistent with the positive shift of the oxidation peak in CVs of PHT films. For both spun and cast films, maximum conductivities for PHT97% and PHT54% films are around 50 and 1 S cm^{-1}, respectively. These values are close to those reported for regioregular and regiorandom PHT films doped with I_2 vapor.[21]

Mobilities for the PHT97%, PHT81%, PHT70%, and PHT54% films, evaluated from combination of the doping level and conductivity data, are plotted against the doping level in Figure 4. The mobility for the cast film of PHT97% is around 2.2×10^{-3} cm^2 V^{-1} s^{-1} at the lowest doping level of 0.028% and

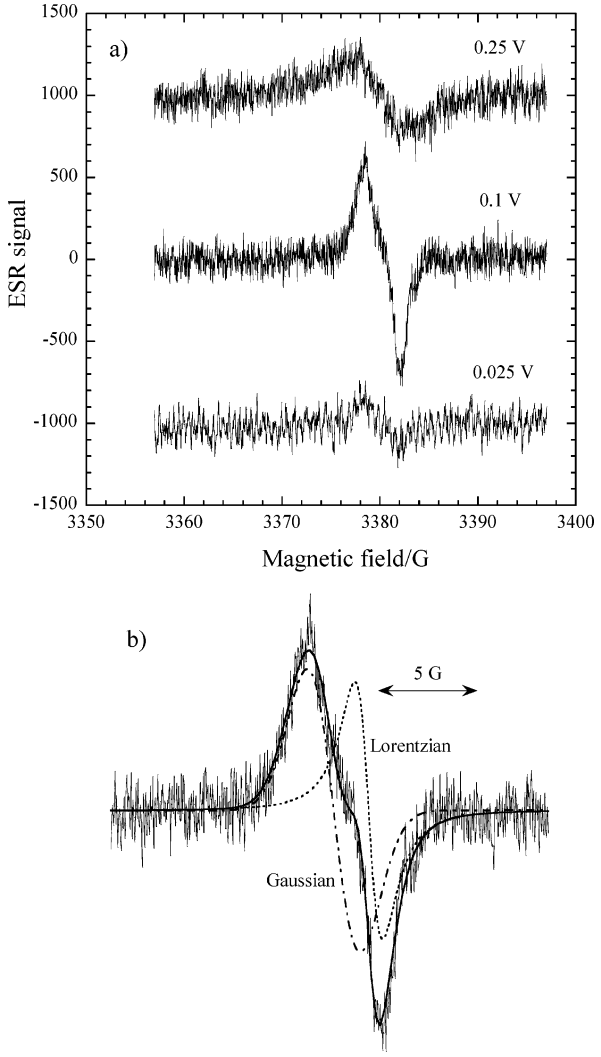

Figure 5. (a) Typical ESR spectra of PHT97% film at different potentials. (b) ESR signal at 0.1 V simulated by a superposition of Gaussian and Lorentzian lines with different *g*-factors.

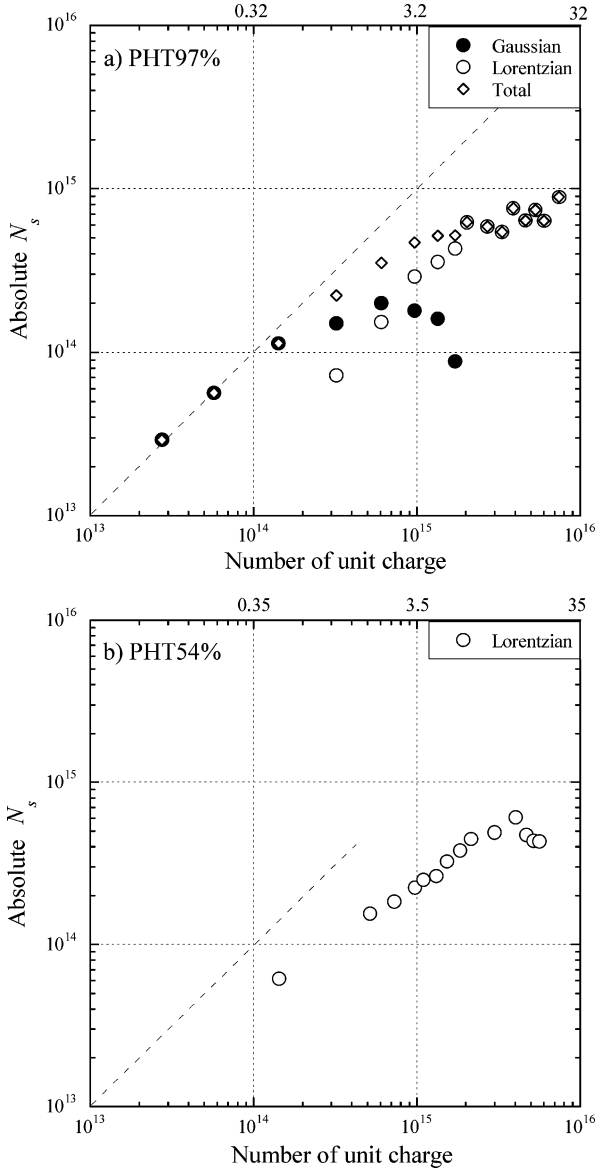

Figure 6. Double logarithmic plots of absolute spin number in (a) PHT97% and (b) PHT54% films for total (●), Gaussian (○), and Lorentzian (△) signals against the number of unit charge.

decreases to reach 8×10^{-4} cm^2 V^{-1} s^{-1} at the 0.4% doping level. The mobility starts to increase strikingly at 1% doping level and reaches 0.37 cm^2 V^{-1} s^{-1}. The mobility for the cast film of PHT54% is around 0.9×10^{-5} cm^2 V^{-1} s^{-1} at the 0.01% doping level and also decreases upon oxidation of the film until it reaches 2.3×10^{-6} cm^2 V^{-1} s^{-1} at the 1.4% doping level. It then starts to increase sharply when the doping level exceeds 2%. For both PHT97% and PHT54%, the mobilities for spun films are comparable with those for cast films, although in the low doping region the mobility for the spun film of PHT97% is slightly lower than that for the corresponding cast film. The decrease of mobility with the increase of doping level in the low doping region and the sharp increase of mobility at doping levels beyond ca. 1% are common features of all the films including PHT81% and PHT70%. We note further that mobility values increase systematically with the increase in regioregularity of PHT.

3.2. In-Situ ESR Measurements. ESR studies were in-situ performed with cast films of PHT97% and PHT54%. Typical ESR spectra of the PHT97% film measured at three different potentials are shown in Figure 5a. It is seen that the ESR signals vary drastically with the applied potential. No ESR signal was detected for a completely dedoped PHT97% film. At a potential of 0.025 V, corresponding to the doping level of around 0.1%, a weak ESR signal fitting a Gaussian line shape with a peak-to-peak line width (ΔH_{pp}) of about 4 G was observed. ESR signals were asymmetric at doping levels of 0.5−4%. As the doping level was increased, the signal became broader and fitted a single Lorentzian line. The signal line shape for the intermediately doped PHT97% film was found to depend on the microwave power, suggesting that there exist at least two different ESR components. These asymmetric signals were well simulated by superposition of Gaussian and Lorentzian lines with different *g*-factors as shown typically in Figure 5b. Double logarithmic plots of absolute spin numbers for Gaussian (N_s^G) and Lorentzian (N_s^L) components, and for a total ESR signal (N_s^T) against the number of unit doping charge as well as the doping level are given in Figure 6a. In the low doping region where only the Gaussian component is observed, N_s^T or N_s^G coincides well with the charge number. N_s^G tends to saturate and then decreases greatly with an increase of doping level. On the other hand, the Lorentzian component becomes appreciable when the doping level is beyond ca. 0.5%. The total spin number N_s^T deviates downward from a straight line with a unity slope as the doping level is increased. The ESR measurements with PHT97% clearly indicate that two kinds of para-

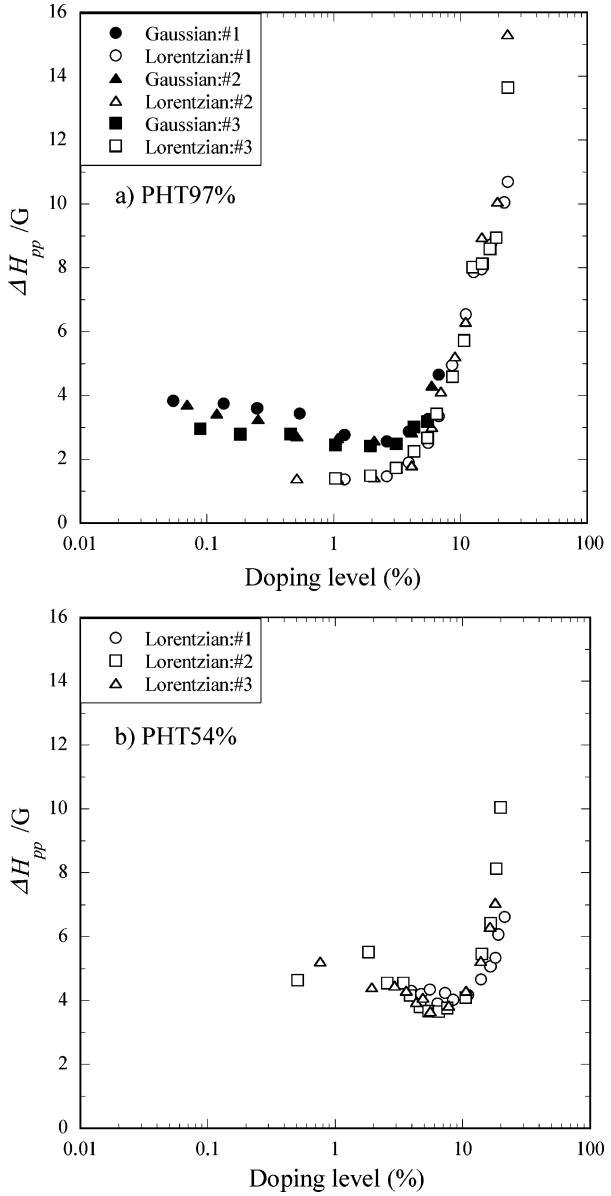

Figure 7. Plots of ΔH_{pp} vs doping level for Gaussian (○, △, □) and Lorentzian (●, ▲, ■) components in (a) PHT97% film and Lorentzian signal (○, △, □) in (b) PHT54% film in three different experimental runs.

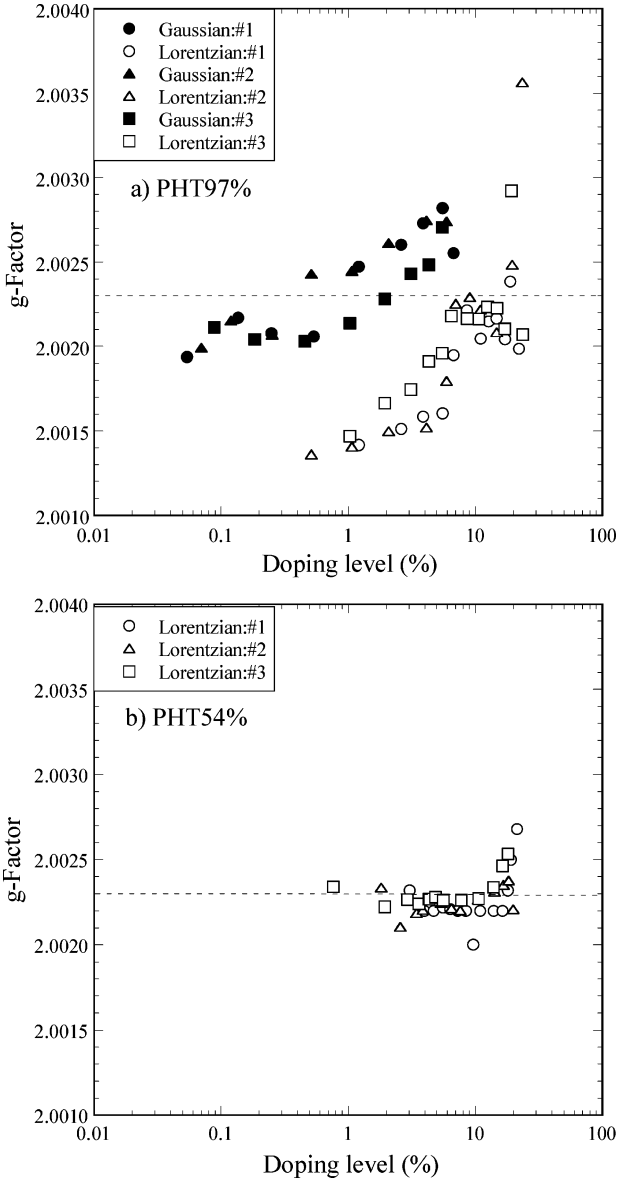

Figure 8. Plots of *g*-factor vs doping level for Gaussian (○, △, □) and Lorentzian (●, ▲, ■) components in (a) PHT97% film and Lorentzian signal (○, △, □) in (b) PHT54% film in three different experimental runs.

magnetic species, most likely polarons, are formed in the PHT97% film and the relative fractions of the two kinds of polarons are varied by the doping level. Moreover, we note that in the intermediate and heavy doping regimes a part of these polarons are transformed to some diamagnetic species.

ESR signals of the PHT54% film, on the other hand, fitted a single Lorentzian line over the entire doping region studied. As shown in Figure 6b, the N_s value of the Lorentzian signal increases with the doping level showing a peak at a doping level of 14%. It is to be noted here that the spin number for the PHT54% film is obviously smaller than the number of doping charge even at the lowest doping level, suggesting that polarons are in equilibrium with diamagnetic species such as bipolarons or π-dimers even in the very lightly doped film.

Figure 7 depicts ESR line widths ΔH_{pp} for the PHT97% and PHT54% films plotted against the doping level. These in-situ ESR measurements were carried out three times for each sample and the results showed completely similar trends for ΔH_{pp}, N_s, and *g* factor. As shown in Figure 7a for the PHT97% film, the ΔH_{pp} value of the Gaussian component decreases slightly at doping levels between 0.07 and 2%, whereas that of the Lorentzian component is almost constant at 1.5 G at doping levels of 0.5−3%. The ΔH_{pp} value for the Lorentzian component starts to increase sharply with an increase in the doping level beyond 4% and reaches 15 G at the highest doping level. The ΔH_{pp} value for the Gaussian component also increases at a similar doping level. As shown in Figure 7b for the PHT54% films, ΔH_{pp} of the Lorentzian signal appears to decrease at doping levels of 1−7% and starts to increase greatly at a higher doping level, being similar to the case of the PHT97% film.

Figure 8 shows *g* factors for the PHT97% and PHT54% films. In Figure 8a for the PHT97%, the *g* factors for the Gaussian component increase slowly with doping level but do not deviate considerably from the free electron value shown by a broken line. The *g* factors for the Lorentzian component are initially around 2.0015, slightly smaller than the free electron value, and then increase with the doping level. As shown in Figure 8b, on the other hand, *g* factors for the PHT54% films are close to the free electron value in the doping range of 1−20%.

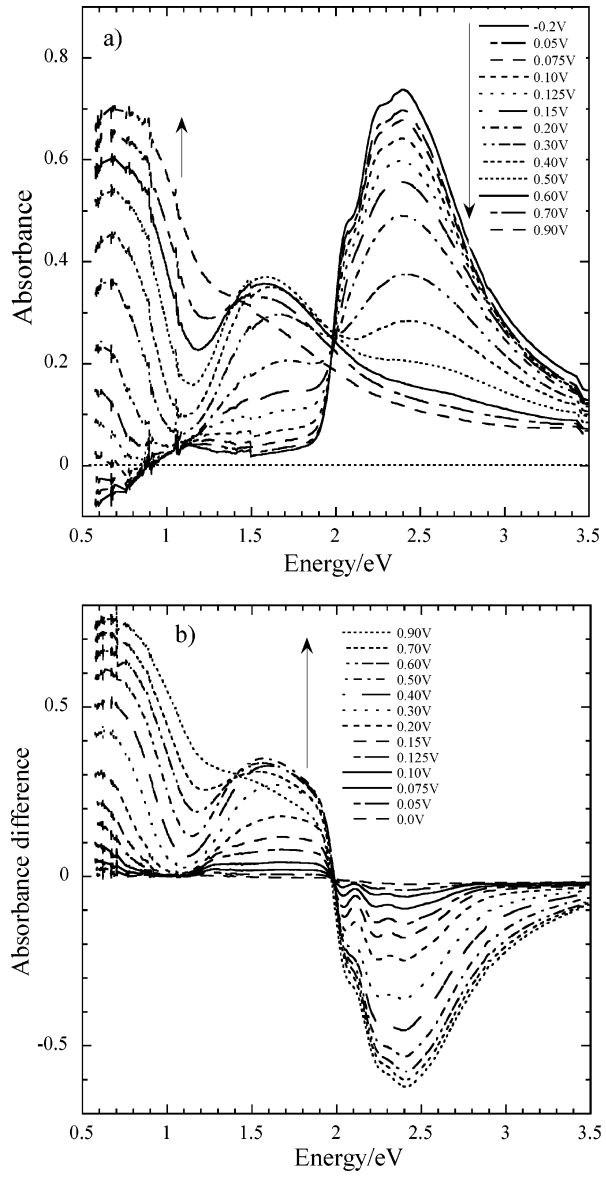

Figure 9. (a) In-situ absorption spectra and (b) difference absorption spectra of a spun film of PHT97% at various potentials.

3.3. In-Situ UV−Vis−NIR Spectroscopy. Absorption spectra of spun films of PHT97% and PHT54% on ITO were taken at different potentials to identify chemical species that are generated at various oxidation stages of the polymer films. As shown in Figure 9a, the interband transition for the neutral PHT97% film appears at around 2.4 eV accompanied by two shoulders at 2.25 and 2.07 eV, in accord with the previous observations for regioregular PAT films.[4,22] When the potential increases beyond 0.15 V, corresponding to the first oxidation peak in CV, the shoulders become obscure and finally disappear. The difference absorption spectra of the PHT97% film shown in Figure 9b indicate that at potentials between 0.0 and 0.075 V (ca. 0.1−1% doping level), two broad but discernible peaks are seen at 1.28 and 1.8 eV along with tailing of a peak below 0.75 eV. These absorption bands are characteristic of polarons.[23−25] As the potential is increased further, the 1.28 and 1.8 eV bands are obscured and another two broad peaks at around 0.65 and 1.65 eV, corresponding to bipolaron bands,[24,25] increase their intensities greatly. At potentials beyond 0.3 V (ca. 5% doping level), the absorption band at 1.65 eV gradually shifts to a lower energy side accompanied with a decrease in intensity, whereas the 0.65 eV band continuously increases with the peak position being almost unchanged.

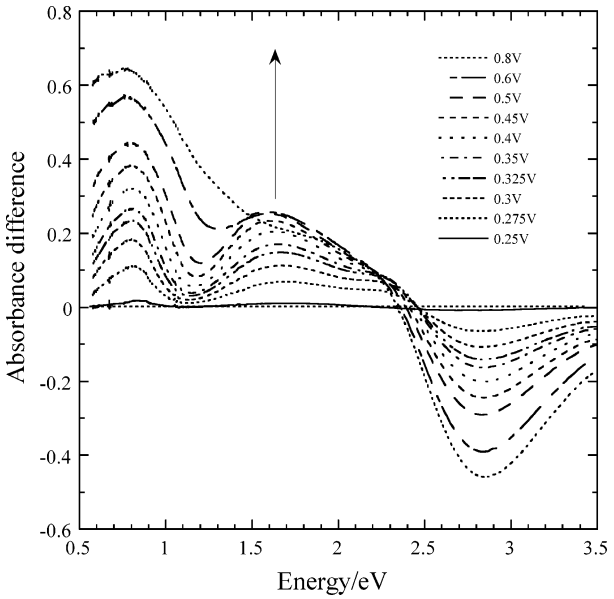

Figure 10. Difference absorption spectra of a spun film of PHT54% at various potentials.

Figure 10 depicts difference absorption spectra of a PHT54% film. A neutral film showed a single broad absorption band at 2.85 eV due to the $\pi-\pi^*$ transition. In contrast to the spectra of the PHT97% film, no absorption bands due to polarons are seen in Figure 10 for the PHT54% film at very low potentials. Instead, two absorption bands at 0.8 and 1.65 eV, ascribable to bipolarons,[24,25] appear and increase gradually as the potential increases. At potentials higher than 0.45 V (ca. 6−7% doping), the 1.65 eV band shifts to a red side and decreases, whereas the 0.8 eV band continuously increases with no change in the peak position, similar to the spectral change of the PHT97% film.

3.4. X-ray Diffraction Measurements. X-ray diffraction measurements were carried out for the spun and cast films of PHT97% and PHT54%. Both spun and cast films of PHT97% showed strong first- and weak second-order reflections at 2θ of 5.4° and 11°. These peaks correspond to an interlayer d spacing of 16.4 Å for the well organized lamellar structure.[26] Diffraction patterns for both spun and cast films of PHT54% measured under the same conditions showed a totally amorphous structure.

4. Discussion

4.1. Characterization of Charge Carriers in PHT Films. Main chains of regioregular PATs in cast and spun films are known to be self-organized due to a regular arrangement of alkyl side chains, resulting in a well-ordered layered structure. It is thus supposed that thin films of regioregular PATs consist of crystallites embedded into a more disordered amorphous phase, whereas regiorandom PATs form only a disordered phase in the film. This view is consistent with the X-ray diffraction measurements made with PHT97% and PHT54% films and explains the difference in CV curves of Figure 1 for the respective films as described below. As for the cast and spun films of PHT97%, main oxidation peaks appear at 0.15−0.2 and 0.5 V. When the film preparation was changed to give uniform and shiny surfaces, the first oxidation peak was greatly enhanced, as shown by curve 3 of Figure 1a. Attainment of the shiny polymer film may be explained by the increase in the

amount of the self-ordered phase in the PHT97% film, and thus peak I can be assigned to oxidation of the ordered phase and peak III to that of the amorphous phase. Peak II is interpreted by Skompska et al. in terms of oxidation of a quasi-crystal region.[27] Indeed, for the PHT54% film comprising only an amorphous phase, no oxidation peak is seen at potentials close to peaks I and II, and only one peak is observed at 0.6 V. A neutral film of PHT97% gives a main absorption band at 2.4 eV together with two shoulders at 2.25 and 2.07 eV. These absorption shoulders, observed only for regioregular PATs, are related to the self-ordered structure of neutral polymer chains[28] and they disappear upon oxidation of the PHT97% film at potentials beyond 0.15 V, corresponding to the potential of peak I in Figure 1a. This finding supports that the polymer chains in the well-ordered domain of the PHT97% film are oxidized at the first oxidation wave in Figure 1a. Systematic decrease of oxidation currents for peak I with the decrease in regioregularity is indicative of the decrease of the well-ordered crystal domain in the PHT films.

ESR measurements with the cast film of PHT97% show the generation of two kinds of paramagnetic species with different *g* values and line shapes. Paramagnetic species with a Gaussian line shape observed in the low doping region are reasonably ascribed to polarons from spectroelectrochemistry and can be considered to be generated by the oxidation of the ordered phase in the PHT97% film. The other paramagnetic species with a Lorentzian line shape are generated at more positive potentials and are ascribable to polarons in the amorphous phase. Single Lorentzian signals are found for the cast film of PHT54%, showing that this polymer film consists solely of the amorphous phase. Polarons in amorphous films of electrochemically synthesized PMT and polyaniline also gave a Lorentzian signal.[20,29] As shown in Figure 6a, Gaussian polarons in the PHT97% film are produced at the same number of doping charges when the doping level is below 0.5%. On the other hand, Lorentzian polarons in the amorphous PHT54% film are less generated than the doping charge even at the lowest doping level of 0.5%. The smaller number of polarons than the number of removed charges can be explained by the generation of diamagnetic bipolarons as evidenced by absorption spectra of Figure 10 for the PHT54% film. Bipolarons are also formed in the PHT97% film as seen from Figure 9 and, more explicitly, from the downward deviation of the N_s^T plot from the straight line shown in Figure 6a. On the basis of the above findings, we are led to the conclusion that polarons in the amorphous phase are less stable than those in the ordered crystal region. This is consistent with the results obtained from the temperature dependence of ESR magnetic susceptibilities made with undoped and iodine-doped samples of regioregular and regiorandom PHTs.[30] The analysis of ESR data has indicated that majority of charges in the regiorandom PHT film is stored as bipolarons and in the regioregular PHT film polarons are only weakly coupled to bipolarons. Molar fractions of paramagnetic and diamagnetic species, by assuming that they are polarons and bipolarons over the whole doping region, are deduced from the doping level vs spin number plots of Figure 6, and the results obtained for the PHT97% and PHT54% films are illustrated in Figure 11. In the low doping regime of the PHT97% film, polarons are predominantly formed in the ordered phase of the polymer film. As the doping level increases beyond 0.2%, their molar fraction decreases monotonically and bipolarons increase their fraction. Polarons in the amorphous phase, on the other hand, start to be created at relatively high doping levels and their molar fraction reaches a maximum. The decrease of the molar fraction beyond the 5% doping level suggests the generation of bipolarons in the amorphous phase of the PHT97% film. In the PHT54% film, polarons are in equilibrium with bipolarons even at the lowest doping level. With the increase in the doping level, the molar fraction of polarons decreases and that of bipolarons increases.

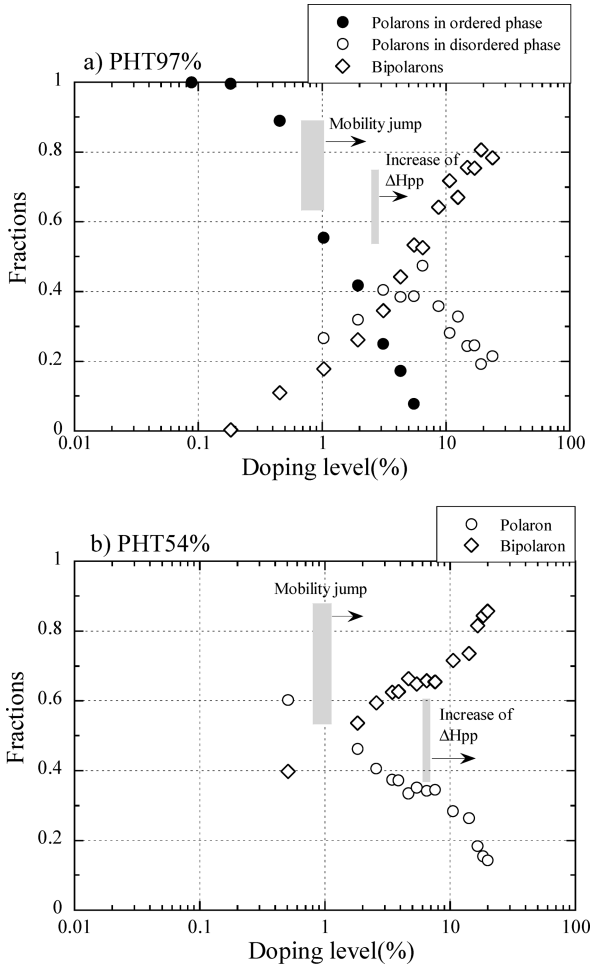

Figure 11. Molar fractions of polarons in ordered phase (●) and amorphous phase (○), and of bipolarons (◊) in cast films of (a) PHT97% and (b) PHT54%. Hatchings represent the onset doping regions for the mobility jump and the ΔH_{pp} increase.

4.2. Charge Transport Mechanisms in PHT Films. According to the composition diagrams shown in Figure 11, polarons in the well-ordered phase are dominant charge carriers in the PHT97% film at doping levels below 0.1%, whereas one can expect that polarons are majority charge carriers in the amorphous PHT54% film at doping levels as low as 0.01%. Therefore, mobility values of 2×10^{-3} and 8×10^{-6} cm^2 V^{-1} s^{-1} for the PHT97% and PHT54% films at doping levels close to ca. 0.01% would represent those of polarons in the well-stacked phase and in the amorphous phase, respectively. Negative slopes of the mobility plots common to all PHT films in the low doping regions will be discussed later. Previous studies by us with a series of copolymers having chemically controlled π-conjugation lengths have shown that polarons do not migrate via an intrachain hopping path, but an interchain route: mobilities of polarons are found to be controlled principally by the rate of hopping of charges between adjacent polymer chains.[18,31,32] Therefore, higher mobilities of polarons in the PHT97% film can be a consequence of facile transport of charges through stacked thiophene rings.

Several mobility studies based on the FET technique have revealed that the increase in regioregularity of PATs leads to the enhancement of mobilities of charge carriers in the PAT films.[7,11−13] The mobility values lie in the range 10^{-2} to 10^{-1} $cm^2\ V^{-1}\ s^{-1}$ for regioregular PATs,[7,11−13] compared with 10^{-5} to 10^{-4} $cm^2\ V^{-1}\ s^{-1}$ for regiorandom PATs.[33−36] Sirringhaus et al. have also found a systematic change of FET mobilities with regioregularity of PHTs: the mobilities for spun films of PHTs with regioregularity of 96%, 91%, 81%, and 70% are 5×10^{-2}, 10^{-2}, 2×10^{-4}, and 2×10^{-5} $cm^2\ V^{-1}\ s^{-1}$, respectively.[7,37] In the present transport study based on electrochemistry, mobility values at the respective lowest doping levels attainable are 2×10^{-3}, 10^{-4}, 2×10^{-5}, and 8×10^{-6} $cm^2\ V^{-1}\ s^{-1}$ for PHTs with regioregularities of 97%, 81%, 70%, and 54%, respectively. The extent of self-ordering and the amount of the ordered domain of PATs are known to be significantly influenced by the film preparation conditions including the kind of solvent, resulting in the variations of mobilities.[7,10] Taking into account the difference in the film preparation technique and the fact that the mobility values given above are the lowest limits for those of neutral PHT films with which FET experiments are performed, the trend of the mobility change found in the present study matches well the one reported by Sirringhaus et al.[7,37]

One of striking features in the doping level vs mobility plots of Figure 4 is an initial decrease of mobility followed by a drastic mobility increase starting at around 1% doping level, which is common to all the PHT films of different regioregularities. The gradual decrease in mobility occurs in the low doping region below 1%, although the decreasing rates are dependent on the kind of PHTs and the film preparation technique, i.e., casting or spin-coating. A similar trend has already been found for spun films of regioregular poly(3-octylthiophene).[16] The mobility decrease in the low doping region was tentatively explained in terms of an increasing fraction of immobile diamagnetic species with the doping level and a scattering of charge carriers by dopant anions. In the cast film of PHT97%, however, no diamagnetic species are generated at doping levels below 0.2%, where the mobility plot has a negative slope. Moreover, it appears to be unlikely that charge carriers, which will move by hopping between adjacent polymer chains, are scattered like free electrons in metals and semiconductors by incorporated dopant anions as impurities. An alternative explanation for the decrease of mobilities is a swelling of the cast films induced by incorporation of anions surrounded by solvent molecules into the polymer film. The swelling of polymer films may take place for electrochemically synthesized conducting polymers to a lesser extent, resulting in no appreciable decrease of mobility as observed for electrosynthesized films of poly(3-methylthiophene) and polythiophene.[14,15] To prove this reasoning, we made preliminary experiments with two types of PHT films. One type of PHT films was prepared by electrochemical oxidation of hexylthiophene monomer and the other type was cast films prepared from a chloroform solution of PHT obtained by dissolution of the former film. Mobility measurements with the two PHT films showed that an initial mobility decrease similar to those in Figure 4 was seen only for the cast film. The results will be reported in detail in our future publication.

Another interesting feature to be discussed is a jump of mobilities at almost the same doping levels of ca. 1% for PHT films with different degrees of orderness. The extent of the mobility jump is 500, 1000, 2500, and 5000 times, respectively, for cast films of PHT97%, PHT81%, PHT70%, and PHT54%, showing that the mobility increase is enhanced systematically by the decrease in orderness. The 1% doping level common to all the PHT films compares well with the doping level at which the second-step increase of mobility was observed for poly(3-methylthiophene) films.[14] This mobility increase was ascribed to the evolution of metallic conduction and the increase of ESR line widths just above the 1% doping level was regarded as a sign of the metallic conduction. As is illustrated in Figure 11, for PHT97% and PHT54% films it is clearly seen that the increase of ΔH_{pp} starts at a doping level higher than the increase of mobility, being more evident for the PHT54% film. The delay of the ΔH_{pp} increase implies that occurrence of charge carriers having a free electron nature as represented by the ΔH_{pp} increase follows the increase of mobility at around 1% doping level. It is worth noting that for the PHT97% film the ΔH_{pp} increase is observed at 3% doping level for both Lorentzian and Gaussian signals, corresponding to ESR signals due to polarons in well-ordered and amorphous phases, respectively. Likewise, Lorentzian signal in the amorphous PHT54% film also exhibits an increase in ΔH_{pp}. Unambiguously, these results of the ΔH_{pp} measurements indicate that the metallic conduction occurs in both ordered and amorphous phases of PHT films. In other words, the stacking structure of polymer chains, which facilitates transport of polarons is not essential to the manifestation of the metallic conduction in conducting polymers, or more explicitly, the charge transport in the metallic conduction region takes place through a single polymer chain, i.e., via an intrachain route. This conclusion is quite sound if we presume that an extensive delocalization of positive charges over a single polymer chain is realized by a conformational change of the polymer chain induced by oxidation such as leading to the extended π-conjugation. It is interesting to note here that the extent of the mobility jump for the PHT54% film is 10 times larger than that for the PHT97% film. This appears to be the result of much lower mobility of polarons in the amorphous PHT film than in the crystalline film and of a relatively small difference of mobilities between the two PHT films at the highest doping stages.

5. Conclusions

It is clearly evidenced through the transport study with PHTs of different regioregularities that the evolution of metallic conduction leading to a sharp increase of apparent mobilities occurs only via the intrachain transport of charge carriers. It is inferred that the charge transport through a single polymer chain is facilitated by oxidation of the polymer chain, resulting in the conformational change leading to the enhanced π-conjugation. Two kinds of paramagnetic species having Lorentzian and Gaussian line shapes are detected in the PHT97% film, and they are ascribed to polarons in the amorphous and crystalline phases, respectively. It is found that mobilities of polarons are greatly influenced by the order level and extent of stacking of π-conjugated thiophene rings, indicative of an interchain route being critical in the transport process of polarons. An initial decrease in the mobility plots common to all the PHT films is explained in terms of swelling of the polymer films due to incorporation of solvated anions upon electrochemical oxidation of the films. Mobility difference between cast and spun films is observed only for PHT97% in the low doping region.

References and Notes

(1) Chandrasekhar, P. *Conducting Polymer, Fundamentals and Applications*; Kluwer Academic Publishers: Boston, 1999.

(2) Scrosati, B. *Applications of Electroactive polymers*; Chapman & Hall: London, 1994.

(3) Roncali, J. *Chem. Rev.* **1992**, *92*, 711−738.
(4) McCullough, R. D.; Lowe, R. D.; Jayaraman, M.; Anderson, D. I. *J. Org. Chem.* **1993**, *58*, 904−912.
(5) McCullough, R. D. *Adv. Mater.* **1998**, *10*, 93−116.
(6) Kaniowski, T.; Luzny, W.; Niziol, S.; Sanetra, J.; Trznadel, M. *Synth. Met.* **1998**, *92*, 7−12.
(7) Sirringhaus, H.; Brown, P. J.; Friend, R. H.; Nielsen, M. M.; Bechgaard, K.; Langeveld-Voss, B. M. W.; Spiering, A. J. H.; Janssen, R. A. J.; Meijer, E. W. *Synth. Met.* **2000**, *111*−*112*, 129−132.
(8) Aasmundtveit, K. E.; Samuelsen, E. J.; Guldstein, M.; Steinsland, C.; Flornes, O.; Fagermo, C.; Seeberg, T. M.; Pettersson, L. A. A.; Inganas, O.; Feidenhans'l, R.; Ferrer, S. *Macromolecules* **2000**, *33*, 3120−3127.
(9) Fell, H. J.; Samuelsen, E. J.; Als-Nielsen, J.; Grübel, G.; Mardalen, J. *Solid State Commun.* **1995**, *94*, 843−846.
(10) Kobashi, M.; Takeuchi, H. *Macromolecules* **1998**, *31*, 7273−7278.
(11) Juska, G.; Arlauskas, K.; Osterbacka, R.; Stubb, H. *Synth. Met.* **2000**, *109*, 173−176.
(12) Aleshin, A. N.; Sandberg, H.; Stubb, H. *Synth. Met.* **2001**, *121*, 1449−1450.
(13) Bao, Z.; Dodabalapur, A.; Lovinger, A. J. *Appl. Phys. Lett.* **1996**, *69*, 4108−4110.
(14) Harima, Y.; Eguchi, T.; Yamashita, K. *Synth. Met.* **1998**, *95*, 69−74.
(15) Harima, Y.; Kunugi, Y.; Yamashita, K.; Shiotani, M. *Chem. Phys. Lett.* **2000**, *317*, 310−314.
(16) Kunugi, Y.; Harima, Y.; Yamashita, K.; Ohta, N.; Ito, S. *J. Mater. Chem.* **2000**, *10*, 2673−2677.
(17) Harima, Y.; Jiang, X.; Kunugi, Y.; Yamashita, K.; Naka, A.; Lee, K. K.; Ishikawa, M. *J. Mater. Chem.* **2003**, *13*, 1298−1305.
(18) Amou, S.; Haba, O.; Shirato, K.; Hayakawa, T.; Ueda, M.; Takeuchi, K.; Asai, M. *J. Polym. Sci., Polym. Chem. Ed.* **1999**, *37*, 1943−1946.
(19) Schiavon, G.; Sitran, S.; Zotti, G. *Synth. Met.* **1989**, *32*, 209−217.
(20) Harima, Y.; Eguchi, T.; Yamashita, K.; Kojima, K.; Shiotani, M. *Synth. Met.* **1999**, *105*, 121−128.
(21) McCullough, R. D.; Tristram-Nagle, S.; Williams, S. P.; Lowe, R. D.; Jayaraman, M. *J. Am. Chem. Soc.* **1993**, *115*, 4910−4911.
(22) Rughooputh, S. D. D. V.; Hotta, S.; Heeger, A. J.; Wudl, F. *J. Polym. Sci., Polym. Phys. Ed.* **1987**, *25*, 1071−1078.
(23) Harbeke, G.; Meier, E.; Kobel, W.; Egli, M.; Kiess, N.; Tosatti, E. *Solid State Commun.* **1985**, *55*, 419−422.
(24) Nowak, M. J.; Spiegel, D.; Hotta, S.; Heeger, A. J.; Pincus, P. A. *Macromolecules* **1989**, *22*, 2917−2926.
(25) Colaneri, N.; Nowak, M.; Spiegel, D.; Hotta, S.; Heeger, A. J. *Phys. Rev. B* **1987**, *36*, 7964−7968.
(26) Chen, T.-A.; Wu, X.; Rieke, R. D. *J. Am. Chem. Soc.* **1995**, *117*, 233−244.
(27) Skompska, M.; Szkurłat, A. *Electrochim. Acta* **2001**, *46*, 4007−4015.
(28) Jiang, X.; Harima, Y.; Yamashita, K.; Tada, Y.; Ohshita, J.; Kunai, A. *Chem. Phys. Lett.* **2002**, *364*, 616−620.
(29) Patil, R.; Harima, Y.; Yamashita, K.; Komaguchi, K.; Itagaki, Y.; Shiotani, M. *J. Electroanal. Chem.* **2002**, *518*, 13−19.
(30) Kahol, P. K.; McCormick, B. J.; Epstein, A. J.; Pandey, S. S. *Synth. Met.* **2003**, *135*−*136*, 343−344.
(31) Harima, Y.; Kunugi, Y.; Tang, H.; Yamashita, K.; Shiotani, M.; Ohshita, J.; Kunai, A. *Synth. Met.* **2000**, *113*, 173−183.
(32) Jiang, X.; Harima, Y.; Zhu, L.; Kunugi, Y.; Yamashita, K.; Sakamoto, M.; Sato, M. *J. Mater. Chem.* **2001**, *11*, 3043−3048.
(33) Assadi, A.; Svensson, C.; Willander, M.; Inganas, O. *Appl. Phys. Lett.* **1988**, *53*, 195−197.
(34) Paloheimo, J.; Kuivalainen, P.; Stubb, H.; Vuorimaa, E.; Lahti, D. Y. *Appl. Phys. Lett.* **1990**, *56*, 1157−1159.
(35) Ohmori, Y.; Takahashi, H.; Muro, K.; Uchida, M.; Kawai, T.; Yoshino, K. *Jpn. J. Appl. Phys., Part 2* **1991**, *30*, L610-L611.
(36) Yoshino, K.; Takahashi, H.; Muro, K.; Ohmori, Y.; Sugimoto, R. *J. Appl. Phys.* **1991**, *70*, 5035−5039.
(37) Sirringhaus, H.; Brown, P. J.; Friend, R. H.; Nielsen, M. M.; Bechgaard, K.; Langeveld-Voss, B. M. W.; Spiering, A. J. H.; Janssen, R. A. J.; Meijer, E. W.; Herwig, P.; de Leeuw, D. M. *Nature* **1999**, *401*, 685−688.